

THE RESPONSE CHARACTERISTICS OF
 $\text{CaF}_2\text{:Mn}$ THERMOLUMINESCENT DOSIMETERS

by 682

ALBERT JOHN ALEXANDER

B.S., Kansas State University, 1969

A MASTER'S THESIS

submitted in partial fulfillment of the

requirements for the degree


MASTER OF SCIENCE

Department of Nuclear Engineering

KANSAS STATE UNIVERSITY
Manhattan, Kansas

1970

Approved by:


Major Professor

L O
2668
T4
1970
A43
C.2

TABLE OF CONTENTS

1.	INTRODUCTION	1
2.	THEORY	4
2.1.	Definition and explanation of terms	4
2.2.	Simple model of TL.	7
3.	EQUIPMENT.	10
3.1.	Dosimeters.	10
3.2.	Reader unit	10
3.3.	Gamma cell.	14
4.	THERMOLUMINESCENT DOSIMETRY.	17
4.1.	Glow curve peaks.	17
4.2.	Partial annealing	17
4.3.	Annealing procedure	22
5.	FADING STUDY	24
5.1.	General	24
5.2.	Primary peak.	24
5.3.	Secondary peak.	26
6.	DETERMINATION OF THE CALIBRATION CURVE	32
6.1.	Necessity	32
6.2.	Equipment and technique	32
6.3.	Experimental procedure.	33
6.4.	Analysis of data and results.	34
7.	SUGGESTIONS FOR FUTURE STUDY	39
8.	ACKNOWLEDGEMENTS	40
9.	LITERATURE CITED	41

**THIS BOOK
CONTAINS
NUMEROUS PAGES
WITH DIAGRAMS
THAT ARE CROOKED
COMPARED TO THE
REST OF THE
INFORMATION ON
THE PAGE.**

**THIS IS AS
RECEIVED FROM
CUSTOMER.**

LIST OF FIGURES

1. Energy band model of a crystal	6
2. Typical glow curve for $\text{CaF}_2\text{:Mn}$	8
3. EG and G model TL-3B thermoluminescent dosimeter reader.	11
4. Block diagram of the EG and G model TL-3B reader	12
5. Typical chart record obtained from EG and G model TL-3B TL dosimeter reader for the TL-31 dosimeter	13
6. EG and G model TL-81B reader head adapter.	15
7. Gammacell-220.	16
8. Typical chart record from EG and G model TL-3B TL dosimeter reader for partially annealed TL-31 dosimeters	19
9. Short term changes in TL-31 dosimeter response with fading time for partially annealed dosimeters	20
10. Short term changes in TL-31 dosimeter response with fading time	21
11. Long term changes in TL-31 dosimeter response with fading time for partially annealed dosimeters	25
12. Long term changes in TL-31 dosimeter response with fading time . .	27
13. Loss of stored signal for secondary glow curve peak.	29
14. Calibration curve for EG and G model TL-31 dosimeters.	37

1. INTRODUCTION

There are a number of ways of detecting and measuring ionizing radiation. The art of determining the radiation dose by measuring the effects of radiation is known as radiation dosimetry and the device used to determine the dose is called a dosimeter. One of the more recent types of dosimeters is the solid state. Certain types of insulator crystals store energy when irradiated with ionizing radiation. Upon being heated to an elevated temperature, they release the stored energy in the form of light. This phenomenon is known as thermoluminescence and the solid state dosimeter is called a thermoluminescent dosimeter, TLD. Thermoluminescent dosimeters have found wide usage in the areas of health physics, space exploration, radiotherapy, and geology, to mention a few.

A list of thermoluminescent dosimeters suggested for use in dosimetry is presented in Spurny (1). Each dosimeter exhibits different characteristics which may make it advantageous for use in some situations and impossible in others. Some generally desirable characteristics listed by Schulman (2) are:

- 1) a high concentration of electron or hole traps,
- 2) high efficiency of luminescence when electrons (or holes) are thermally released and recombine with holes (or electrons),
- 3) long storage of trapped electrons or holes at normal working temperature,
- 4) a simple trap distribution for greatest simplicity of operation and reading interpretation,

- 5) a luminescence spectrum which matches the detector and is separated as far as possible from the incandescent emission of the heating source,
- 6) stability of the phosphor to radiation (i.e., radiation should fill the traps but not create or destroy traps).

Spurny (1) also lists the following:

- 1) no excitation of phosphor other than by radiation,
- 2) linear response over range of dose,
- 3) cheap and reproducible production of the phosphor material.

Although TLD can now be considered a well-established technique, the fundamental theory is far from understood. There are also some drawbacks associated with the TLD which need to be solved. The two main drawbacks are:

- 1) The impurity concentration is extremely important in the response of the TLD. Even minute changes in the impurity will drastically affect the characteristics of the TLD. In perspective of this fact, it is extremely difficult to reproduce the phosphors and obtain the same properties.
- 2) The dosimeter readout devices are complicated and expensive.

The thermoluminescent dosimeters used for this research were the externally heated needle dosimeters of $\text{CaF}_2:\text{Mn}$. The $\text{CaF}_2:\text{Mn}$ dosimeter has a high radiation sensitivity and a relatively simple distribution of

stable trapping centers. It also has most of the other desirable characteristics listed above.

There were three main areas to be investigated in this research. First, a study was made on the effects of partially annealing the dosimeters before reading them out to see if the spread of the data could be reduced. Second, a fading study was done to see if previous fading studies could be reproduced and if partial annealing would improve the fading characteristics. Third, a calibration curve was experimentally determined. Some of the things of interest to be resolved while determining the calibration curve were the extent of supralinearity, if any, and the point of saturation. It was hoped that this research would be important in gaining new insights of the thermoluminescence phenomenon.

2. THEORY

2.1. Definition and Explanation of Terms

2.1.1. Roentgen (R):

The basic unit for expressing the biological dose due to gamma rays is the roentgen, defined as: "One roentgen is an exposure dose of x or gamma radiation such that the associated corpuscular emission per 0.00129 g of air produces, in air, ions carrying one electrostatic unit of quantity of electricity of either sign." (3)

2.1.2. Radiation Absorbed Dose (rad):

The rad is another unit of radiation. One rad of absorbed dose is equivalent to 100 erg absorbed per gram where the material is not specified in the definition but is the material in which the absorption occurs. This is probably the more useful unit for TLD work since it is indicative of the energy absorption causing the particular responses. The conversion factor for converting dose in roentgens to dose in rads absorbed in $\text{CaF}_2:\text{Mn}$ is 0.868 (4).

2.1.3. Radiation Thermoluminescence:

This definition was given in the introduction but will be repeated here for completeness. Certain types of crystals store energy when irradiated by ionizing radiation. Upon being heated to an elevated temperature, they release the stored energy in the form of light emission.

This phenomenon is known as thermoluminescence, TL.

2.1.4. Phosphor:

A phosphor is a material which exhibits the thermoluminescent property. If the phosphor is used to determine the total accumulated dose, it is called a dosimeter.

2.1.5. Traps:

An ideal crystal is one which has no imperfections. Extensive studies have shown, however, that real crystals do have imperfections; therefore, they do not attain an ideal structural form. There are a number of possible imperfections and the reader is referred to Schulman's survey article (2). These imperfections cause localized centers of positive or negative charges which are capable of trapping electrons or holes, respectively. These centers are called traps. Some of the more common are the 'F' center (after the German word for color center: "Farbzentrum") and the 'H' center. The 'F' center is a hole trapped by an interstitial anion. The trap population may be greatly enhanced by impurity doping which is also covered by Schulman (2).

2.1.6. Trap Depth:

An ideal crystal cannot have any electrons whose energy states lie in the forbidden energy gap, hence the name forbidden energy gap. The traps, discussed above, have energy states that lie in the forbidden energy gap. The way the electron gets from the trap to the valence band is for its

energy to be raised to that of the conduction band and then it can cascade to the valence band. Thus, the energy it takes to release the electron from a trap corresponds to the trap depth. The deeper the trap, the more energy necessary to free the trapped electron. The difference in the energy states of the conduction band and the trap energy state is called the trap depth, E_t , and is the energy needed to free the trap.

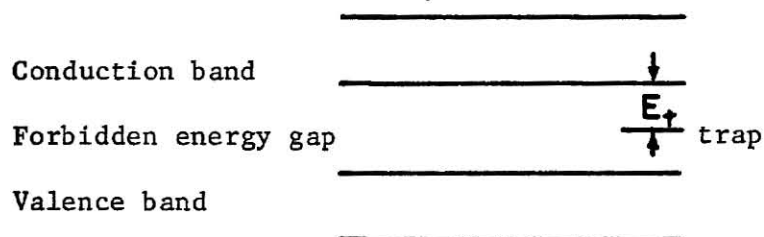


Figure 1. Energy band model of a crystal.

The trap depth for a hole is defined similarly. It is the energy necessary to release a hole from an 'H' center, for example. The number of different trap energy states depends upon the crystal in question. $\text{CaF}_2\text{:Mn}$ is reported to have a relatively simple distribution of stable trapping centers (5).

2.1.7. Glow Curve:

The trap depth, E_t , is directly related to the temperature needed to release the electrons from the traps. As the temperature increases, the

probability of releasing a trap increases until at a certain temperature the electron is released from the trap. The light emitted when the electron cascades back to the valence band (TL) will thus start out weak, go through a maximum, and decrease again to zero. The graph of TL as a function of the time or the temperature is called a glow curve. A typical glow curve as given by Schulman (2) is reproduced in Fig. 2.

2.2. Simple Model of TL

Although the physical and chemical theory of TLD is not known, the basic phenomenon is qualitatively understood. Ionizing radiation upon interacting with an insulating crystal imparts enough energy to electrons to remove them from the valence band to the conduction band. This leaves holes in the valence band. The electrons and holes wander through the crystal until they are trapped in a metastable state or the electrons lose enough energy by collision and fall back into a hole in the valence band (recombination). These metastable states are assumed to be associated with lattice defects caused by natural imperfection or impurity doping of the crystal. There are two ways in which the TL photon may be emitted, depending upon whether the electron or the hole is less stable. Either way, the two processes are similar and it will be assumed the electron trapped is the less stable. When the dosimeters are heated, a temperature is finally reached at some time such that the electron acquires enough vibrational energy to escape from the trap. The electron may now either be trapped again or lose enough energy and fall or cascade back to the valence band emitting one or several

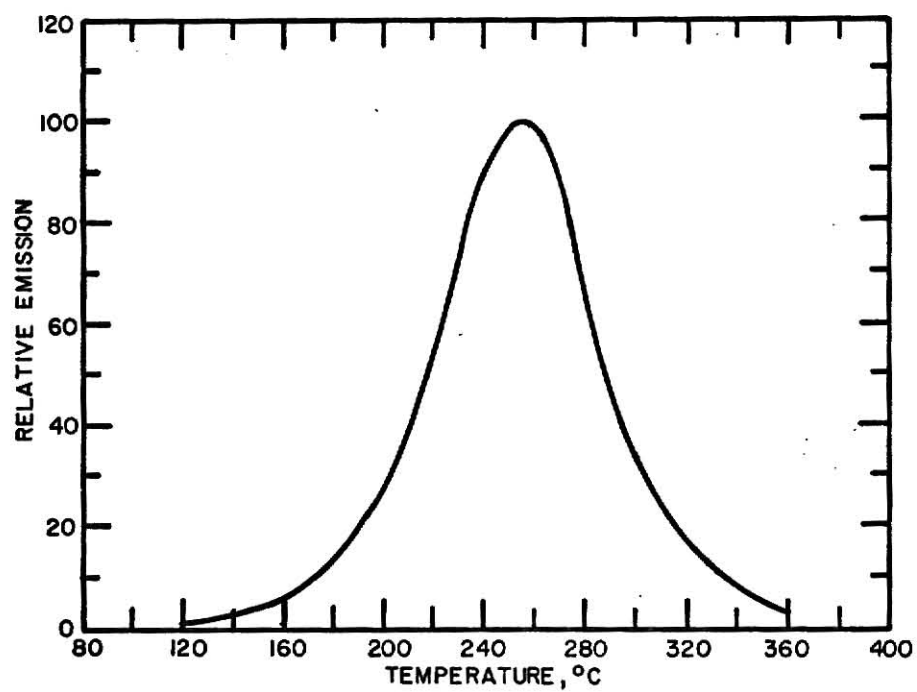


Figure 2. A typical glow curve for $\text{CaF}_2:\text{Mn}$.

photons (TL). The first possibility is of little importance because the probability of this reaction is small in comparison to that of the electron falling back to the valence band and emitting a photon; thus it is usually neglected. This is only a sketchy explanation and the reader is referred to a more complete explanation in Schulman (2).

3. EQUIPMENT

3.1. Dosimeters

The type of miniature dosimeters used in this study was the TL-31 supplied by EG and G, Inc. They contained about 10 mg of calcium fluoride powder doped with manganese, $\text{CaF}_2\text{:Mn}$. This powder was sealed in a glass capillary 1.4 mm in diameter and 12 mm in length.

The reported range on the $\text{CaF}_2\text{:Mn}$ mini dosimeter is from approximately 20 mR to 5×10^5 R. The response is only slightly energy dependent. The temperature dependence is negligible at ambient temperatures. Linearity is reported as 3% over total dose range with a reproducibility of $\pm 3\%$.

There are small inconsistencies in the weight of phosphor, grain size, geometry of ampule, and phosphor sensitivity, but the response of the dosimeters from a batch selected by the manufacturer was supposed to be within $\pm 10\%$ of the mean.

3.2. Reader Unit

An EG and G model TL-3B thermoluminescent dosimeter reader was used to read out the dose incurred by the dosimeters (see Fig. 3). A block diagram is presented in Fig. 4.

The normal range for the reader is 5 mR to 5 kR but the range can be extended up to 50 kR by adjusting the gain on the PM tube.

An illustration of a chart record is presented in Fig. 5. Each time the chart recording pen reached the uppermost value of the scale, the automatic ranging circuit lowered the reader sensitivity by a factor of 10.



Figure 3. A view of the EG and G model TL-3B thermoluminescent dosimeter reader.

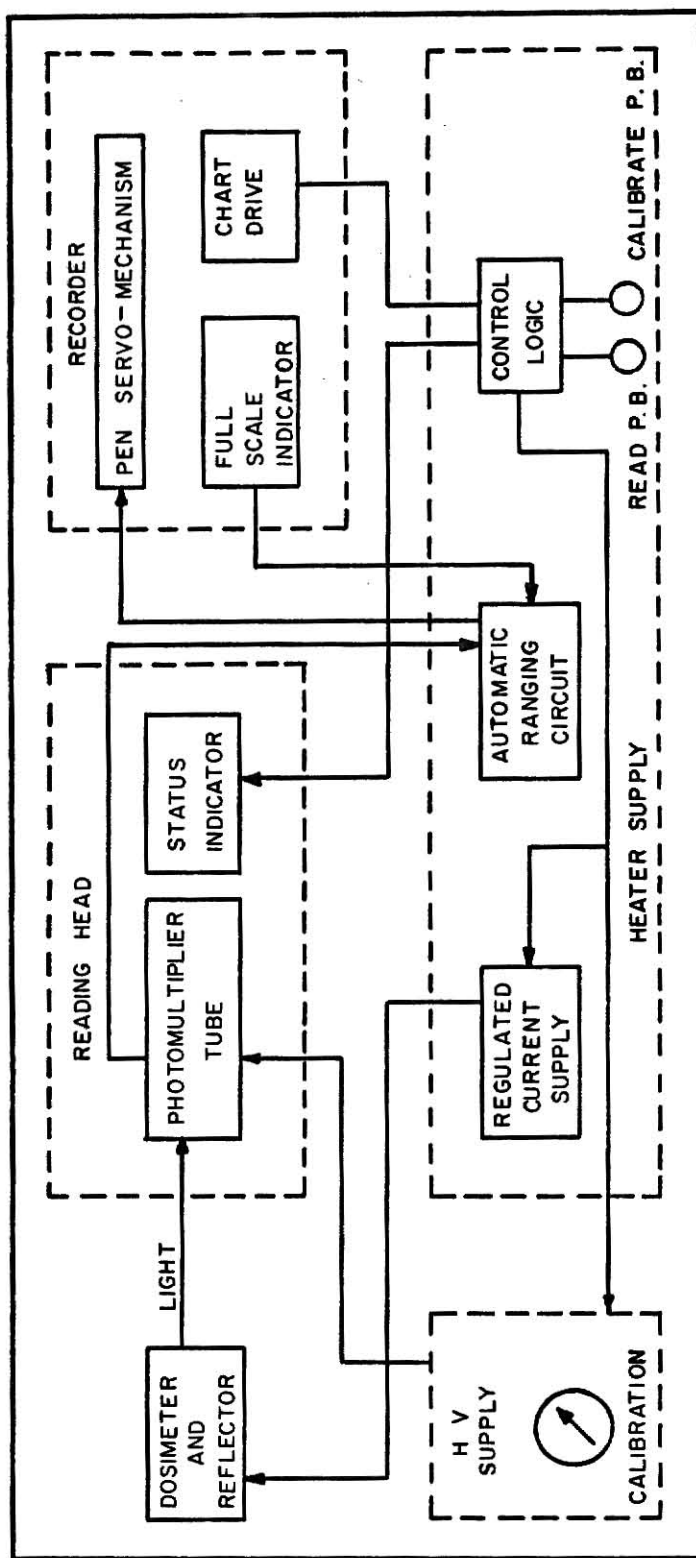


Figure 4. A block diagram of the EG and G model TL-38 reader.

A, CALIF. CHART TL-83 PRINTED IN U.S.A.

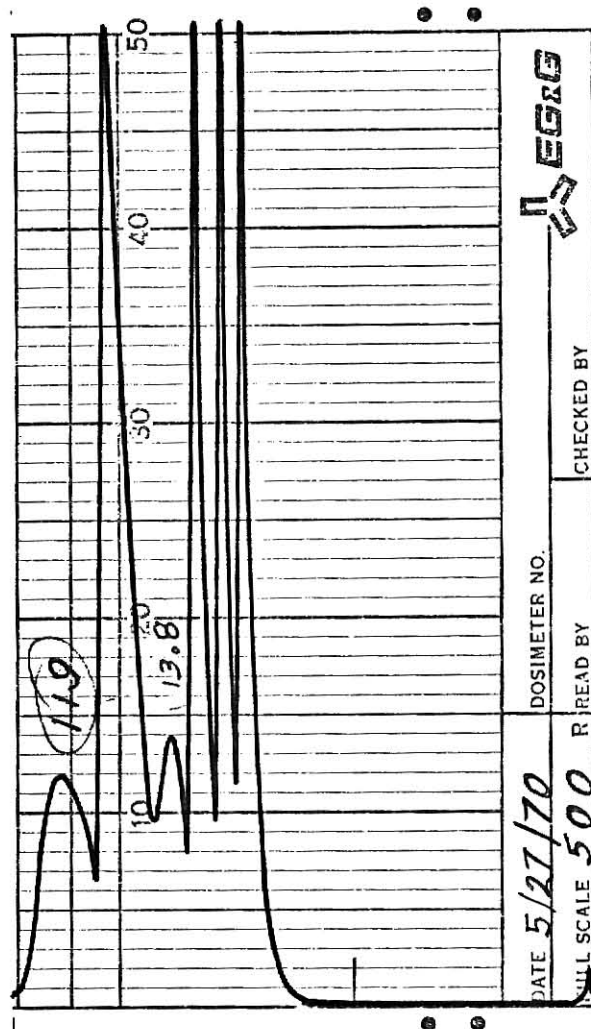


Figure 5. A typical chart record obtained from the EG and G model TL-3B TLD dosimeter reader for the TL-31 dosimeter.

The final full scale reading is indicated in the status window and can be checked by counting the number of scale changes that were necessary.

The EG and G model TL-81 B reader head adapter was used (see Fig. 6) in conjunction with the reader unit to hold and heat the dosimeters. The adapter consisted of a heating coil and a shunt resistance. It received a constant current of 6.5 A from the current supply. This shunt resistor could be adjusted such that the correct amount of current flowed through the resistor so the primary peak occurred in the middle of the three lines to the left of the chart (see Fig. 5).

For a standard reference of setting the high voltage across the PM tube, a ^{14}C source was used to reproduce a 340 mR reading.

3.3 Gamma Cell

A Gammacell-220 of Atomic Energy of Canada, Ltd., was used to irradiate the dosimeters. The gamma-cell was loaded with a 3,963 Ci ^{60}Co source on March 15, 1965. The correct dose rate at the time of irradiation was read from a chart associated with the gamma-cell. The source is in the form of a hollow circular cylinder located inside a thick, water shield. A 6-inch diameter by 8-inch irradiation chamber was located in a plunger, which took it down in the middle of the source. The plunger was operated by an electronic timer which could be set for seconds, minutes, or hours. The Gammacell-220 is shown in Fig. 7.

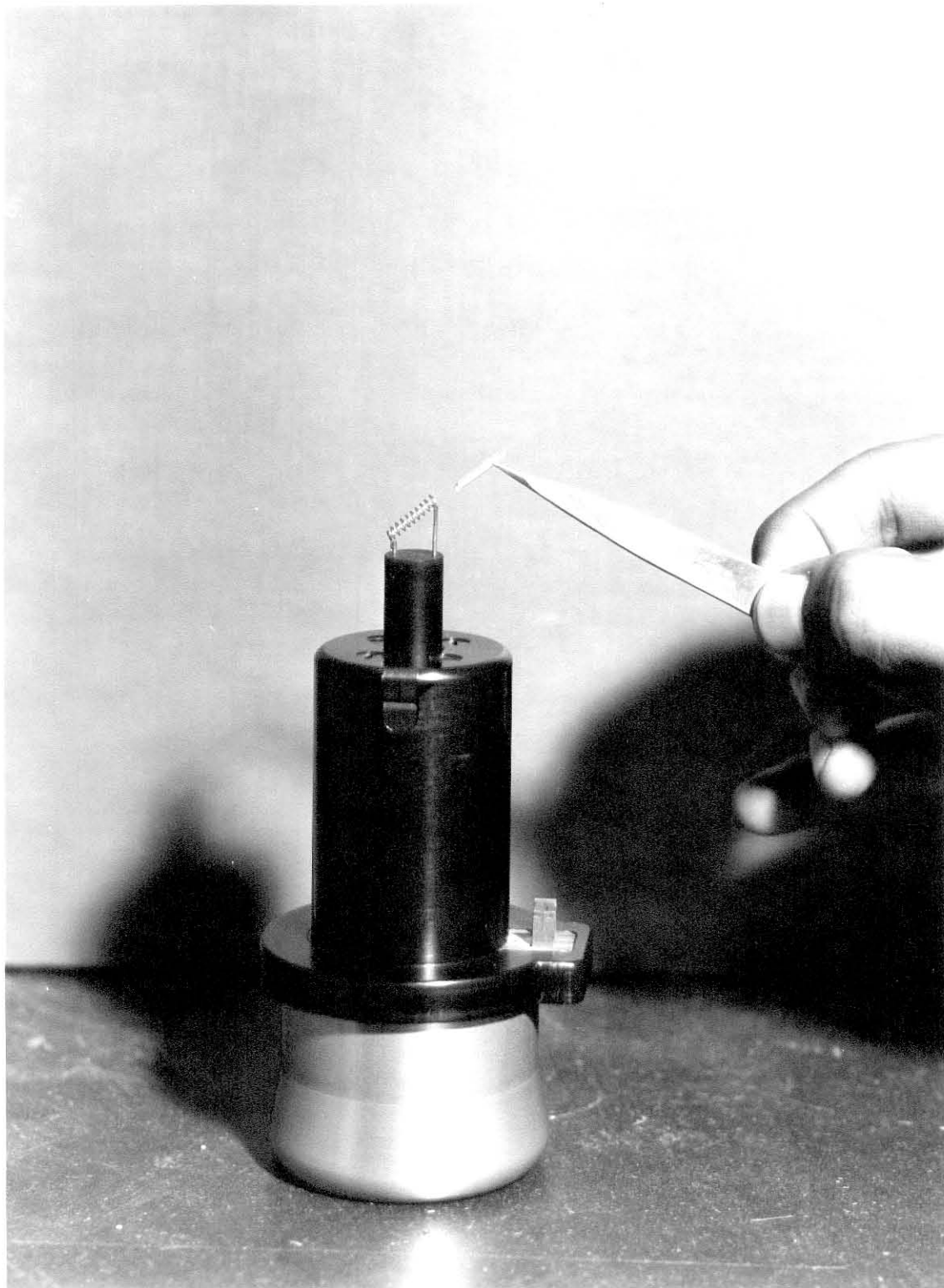


Figure 6. EG and G model TL-81B reader head adapter. Also shown is a model TL-31 dosimeter held in a pair of tweezers.



Figure 7. A view of the Gammacell-220.

4. THERMOLUMINESCENT DOSIMETRY

4.1 Glow Curve Peaks

A typical glow curve as cited in the literature was shown in section 2.1., Fig. 2. From this glow curve, only a single peak occurs. For the EG and G TL-31 dosimeters, a secondary peak was observed in addition to the primary peak. The source of this extra peak is not known but was present in all the EG and G TL-31 dosimeters used in this research. It is suspected that some minute impurity doping may be the source. This extra secondary peak is shown in section 3.2., Fig. 5. This chart recording, shown in Fig. 5, has several changes in scale where Fig. 2 does not; but it vividly exemplifies the two peaks.

The secondary peak may affect the fading properties of the primary peak. The secondary peak has a low trap depth and will easily fade at room temperature. As it fades, it can perceptibly feed the deeper traps.

4.2. Partial Annealing

Kaiseruddin (7) investigated partial annealing effects on TL-21 (LiF Miniature Dosimeters) to eliminate some of the randomness created by the fading of the secondary peak. His technique was to partially anneal the phosphor for seven minutes at 5°C above the excitation temperature of the secondary peak he wanted eliminated before reading them out.

The heating rate for the TL-3B reader is linear, so linear interpolation on the glow curve was used to find the temperature at which the secondary

peak occurred. By assuming the primary peak occurs at 260°C, linear interpolation gives a temperature of 156°C for the secondary peak.

Partial annealing was tried on the TL-31 dosimeters. The partial annealing was at 161°C for 7 minutes. The dosimeters were immediately withdrawn from the annealing oven and left to cool at room temperature for 30 minutes before being read out. This removed the secondary peak as seen in Fig. 8 for the EG and G TL-31 dosimeters.

Sixty-four dosimeters were irradiated to a dose of approximately 640 rads and partially annealed in the previously described manner. They were read out, eight at a time, over a 48-hour time period. Another sixty-four dosimeters were irradiated to a dose of approximately 640 rads and were read out, eight at a time, over a 48-hour time span. The results are presented in Figs. 9 and 10, respectively. An F test was performed to see if the difference in the residuals was significant. The F value is given as (8):

$$F(f_1, f_2) = \frac{s^2}{s_a^2} \quad (1)$$

where

$$s^2 = \frac{\sum_{i=1}^n (y_i - \bar{y})^2}{n - 1}, \text{ estimate of the variance for the dosimeters that}$$

were not partially annealed,

\bar{y} = the mean value of the response for the dosimeters that were not partially annealed,

A, CALIF.

CHART TL-83

PRINTED IN U.S.A.

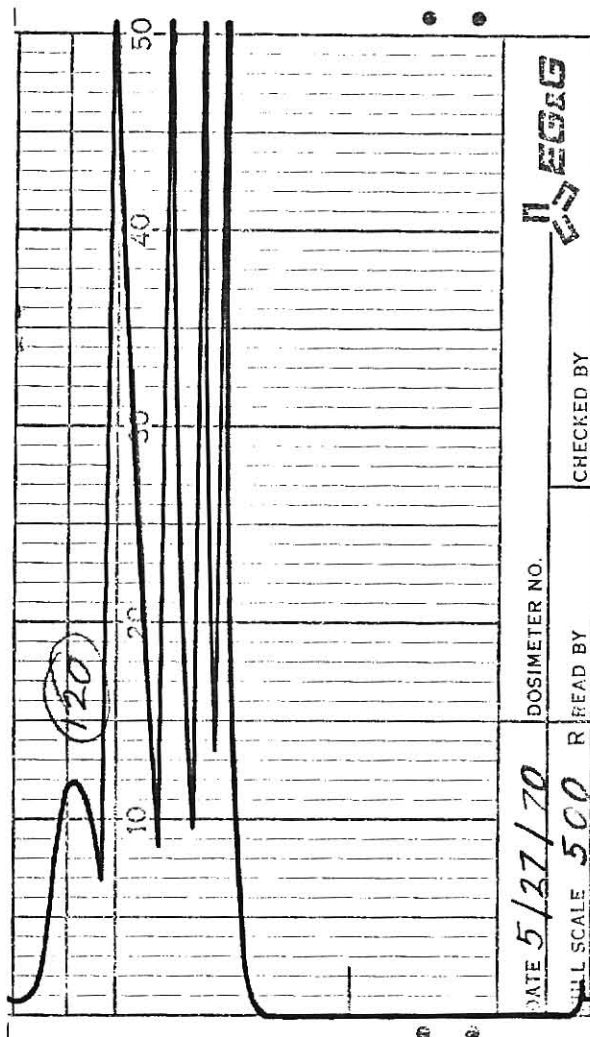


Figure 8. A typical chart record obtained from the EG and G model TL-3B TL dosimeter reader for the partially annealed TL-31 dosimeters.

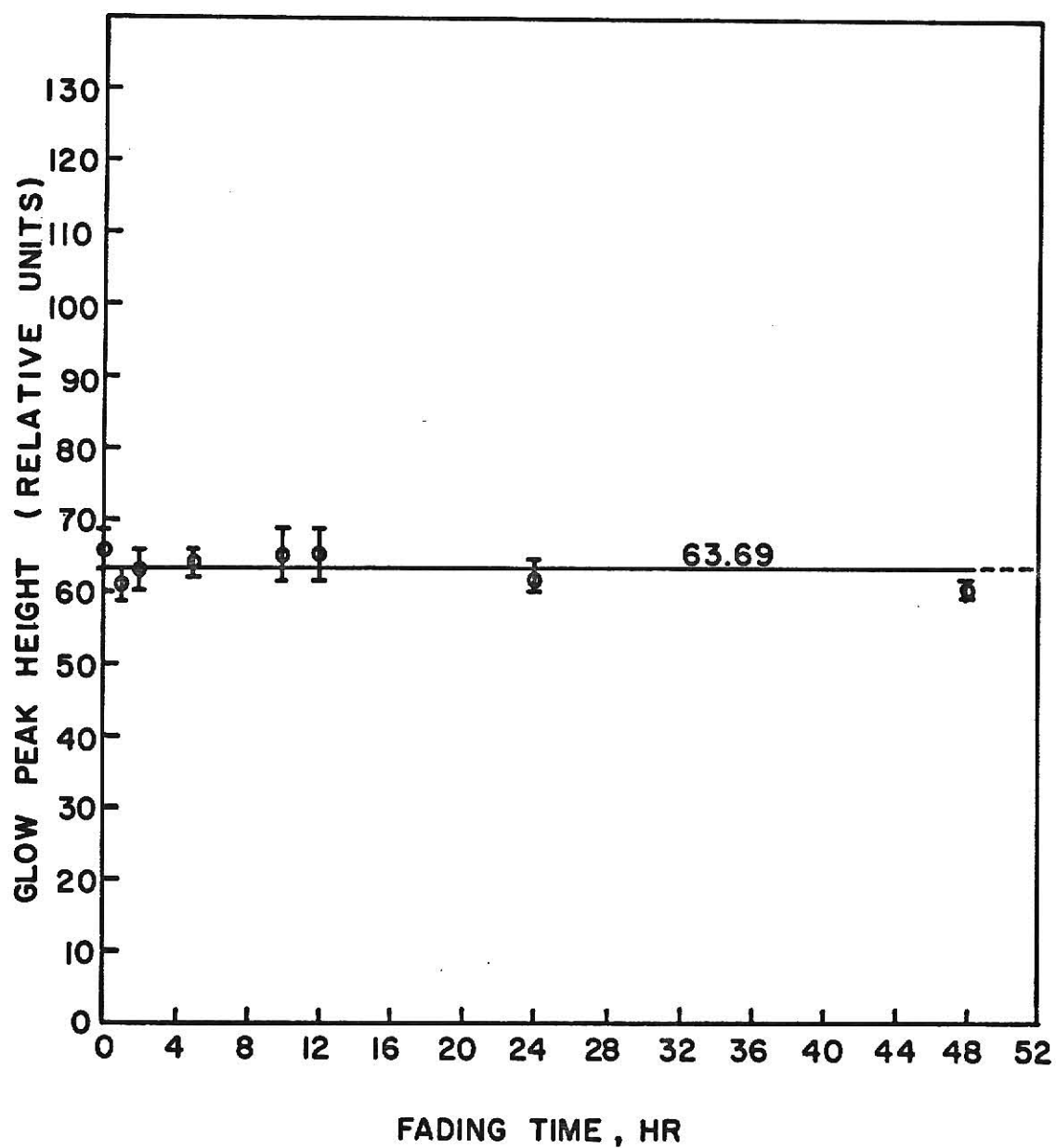


Figure 9. Short-term changes in the dosimeters (EG and G model TL-31) response with fading time. The dosimeters were partially annealed after irradiation at 161°C for 7 minutes.

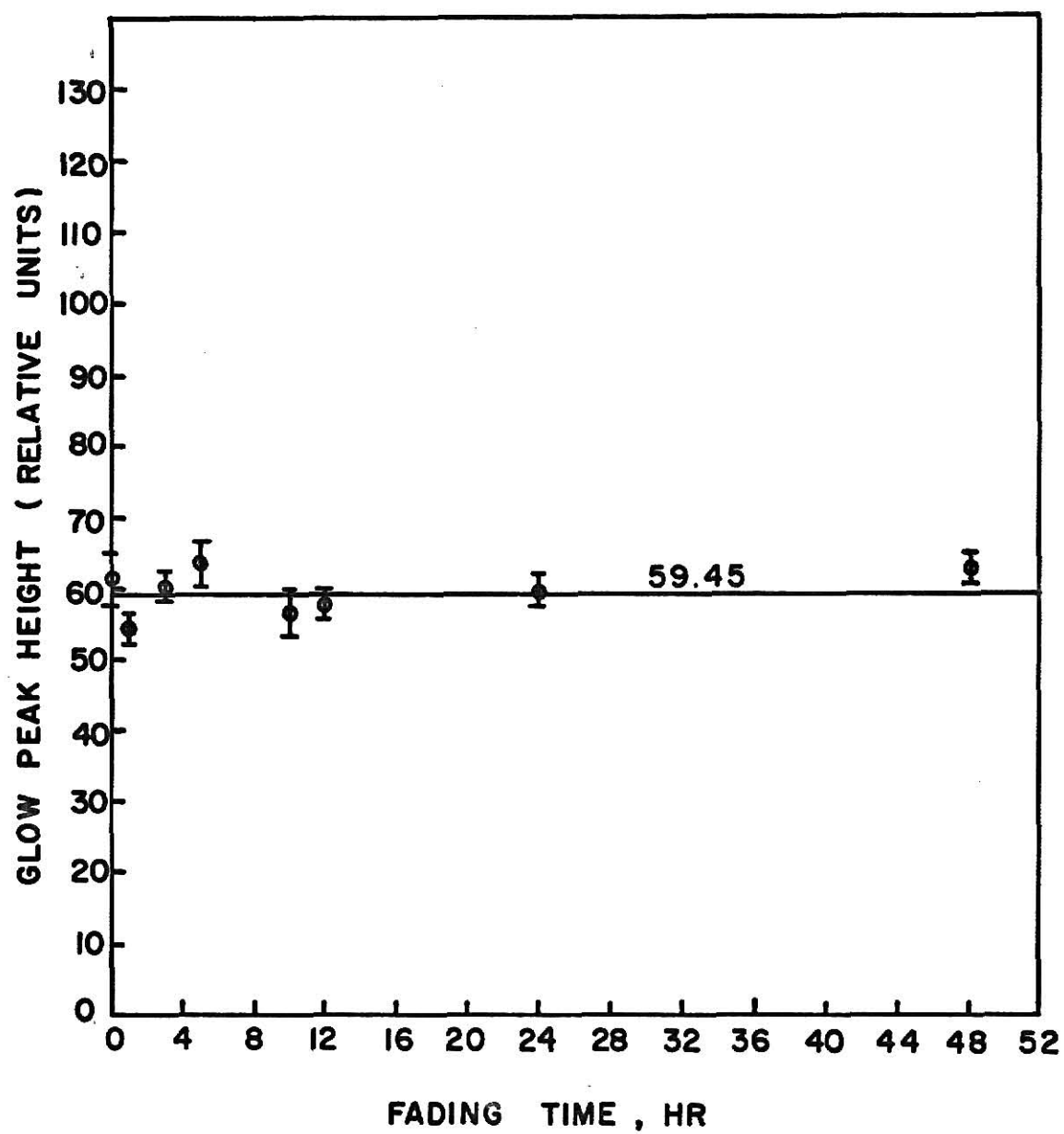


Figure 10. Short-term changes in the dosimeters (EG and G model TL-31) response with fading time.

y_i = the response of the dosimeters that were not annealed,

$s_a^2 = \frac{\sum_{i=1}^n (y_i^a - \bar{y}_a)^2}{n - 1}$, estimate of the variance for the partially annealed dosimeters,

\bar{y}_a = the mean value of the response for the annealed dosimeters,

y_i^a = the response for the partially annealed dosimeters,

n = number of data points,

f_1 = degrees of freedom associated with the s^2 ,

f_2 = degrees of freedom associated with the s_a^2 .

The calculated $F(7,7)$ value was 2.33, which is the value of the critical F , F_c , at 85% confidence level, i.e., at the level of significance, $\alpha = 0.15$. From this test, it was decided that the partial annealing was beneficial to increasing the precision, i.e., decreasing the spread of the data.

4.3. Annealing Procedure

For large doses, all the traps are not fully emptied by the small heating cycle used for reading the dosimeters out. It is necessary to anneal the dosimeters at an elevated temperature for a prolonged time span.

EG and G has a suggested annealing procedure for $\text{CaF}_2:\text{Mn}$ (9). If the previous exposure was large, bake in an oven at 350°C . The following time schedule is recommended:

<u>Dose Range</u>	<u>Time at 350°C</u>
0 mR to 50 mR	0
50 mR to 500 mR	5 minutes
500 mR to 5 R	10 minutes
5 R to 50 R	15 minutes
50 R to 500 R	45 minutes
500 R to 5,000 R	2 hours
5,000 R to 50,000 R	5 hours

The signal from a completely annealed detector should be less than 0.5 mR. If the signal is greater than this, further anneal treatment is indicated.

5. FADING STUDY

5.1. General

Fading of TLD's is due to the annealing of some of the low energy traps at room temperature. A desirable phosphor has a TL response that is fairly independent of time. Thus, the phosphor can be stored at room temperature after exposure and read out at a later date. Phosphors with this characteristic have peaks that occur at relatively high temperatures on the glow curve. In the case of $\text{CaF}_2:\text{Mn}$, the peak occurs at a relatively high temperature of 260°C (6). This would tend to indicate that very little fading should occur.

5.2. Primary Peak

A fading study was done on the primary peak at room temperature. The dosimeters were irradiated to approximately 640 rad. They were then partially annealed at 161°C for 7 minutes. The dosimeters were then read out, eight at a time, over a seven-week time span (see Fig. 11).

These data were analyzed by the standard least squares method. A slope of $0.0056 \pm .0018$ (relative units/hour) was obtained. An analysis of variance was done for the linear regression (8). Under the null hypothesis that the slope is equal to zero, the variance ratio is distributed as $F(1,12) = 10.05$ which is significant at 95 percentage points. Thus, if one sets the level of significance at $\alpha = .05$, the null hypothesis is rejected. This says the slope is positive and different from zero.

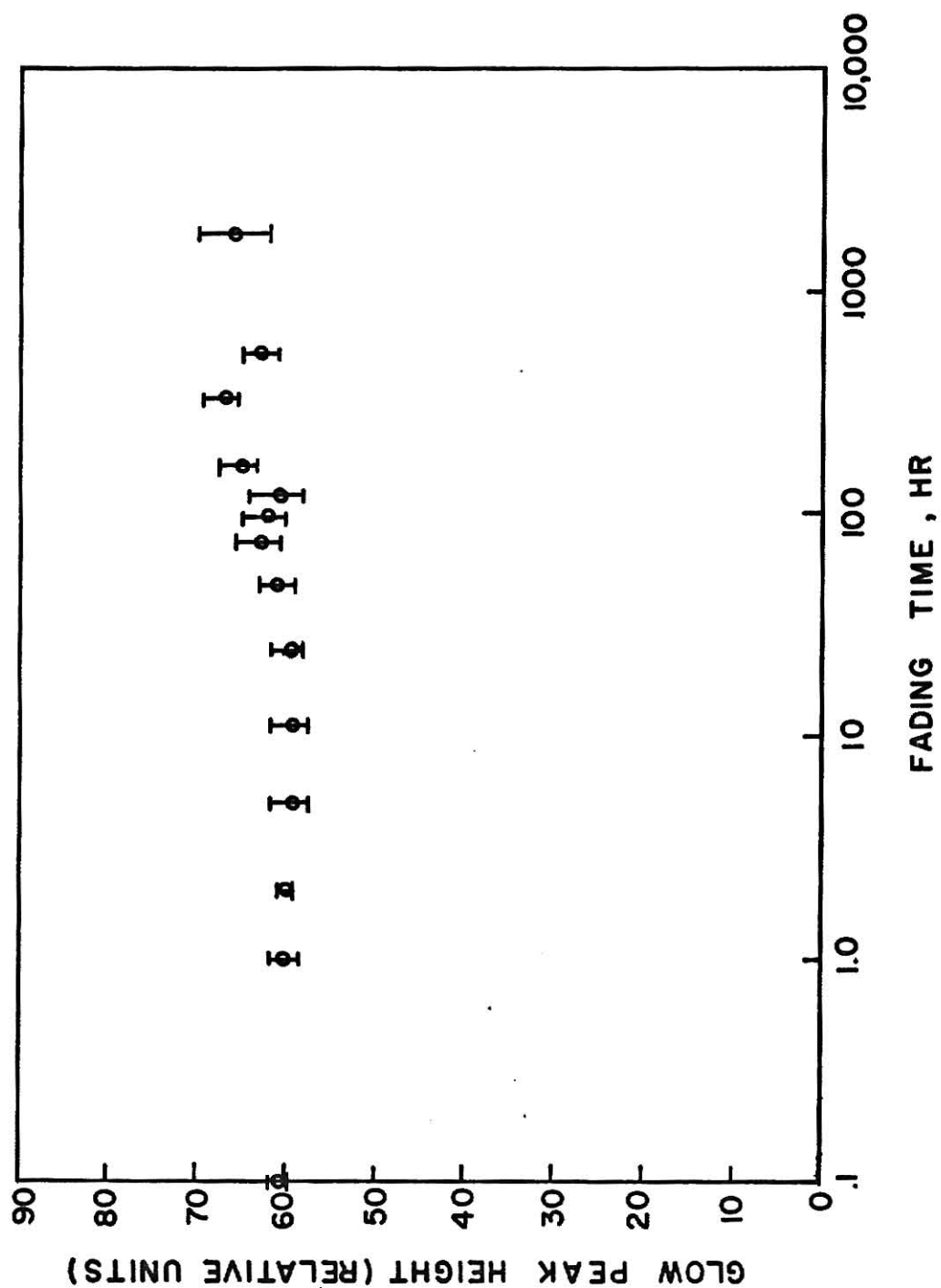


Figure 11. Long-term changes in the dosimeter (EG and G model TL-31) response with fading time. The dosimeters were partially annealed after irradiation at 161°C for 7 minutes.

The fading study was repeated for the primary peak at room temperature; however, this time the dosimeters were not partially annealed. The fading study was over a period of four weeks (see Fig. 12). The value obtained for the slope was $.0021 \pm 0.0042$ (relative units/hour). The deviation on the slope is larger than the slope, which indicates the slope is probably equal to zero.

From the analysis of the variance table, the F value of $F(1,11) = .245$ is small and indicates it is not significant. Thus, it may be assumed that the slope is zero and no fading occurs.

Schulman (2) reported a 10% fading for $\text{CaF}_2:\text{Mn}$ over the first month. In the two fading studies performed here for the primary peak, no fading was observable. The discrepancy between the two can probably be attributed to differences in impurity doping. When dealing with impurity doping properties, only minute changes in the doping procedure or impurity may affect the property of the dosimeters.

5.3. Secondary Peak

As mentioned in section 4.1., a secondary peak was observed with the TL-31 dosimeters. A fading study at room temperature was done on this secondary peak. A batch of dosimeters was irradiated to approximately 640 rad. They were then read out, eight at a time, over a one-week period. Continuing the fading study over a longer time span was not practical since the secondary peak had decayed significantly.

These data points were plotted on semi-logarithmic paper as seen in

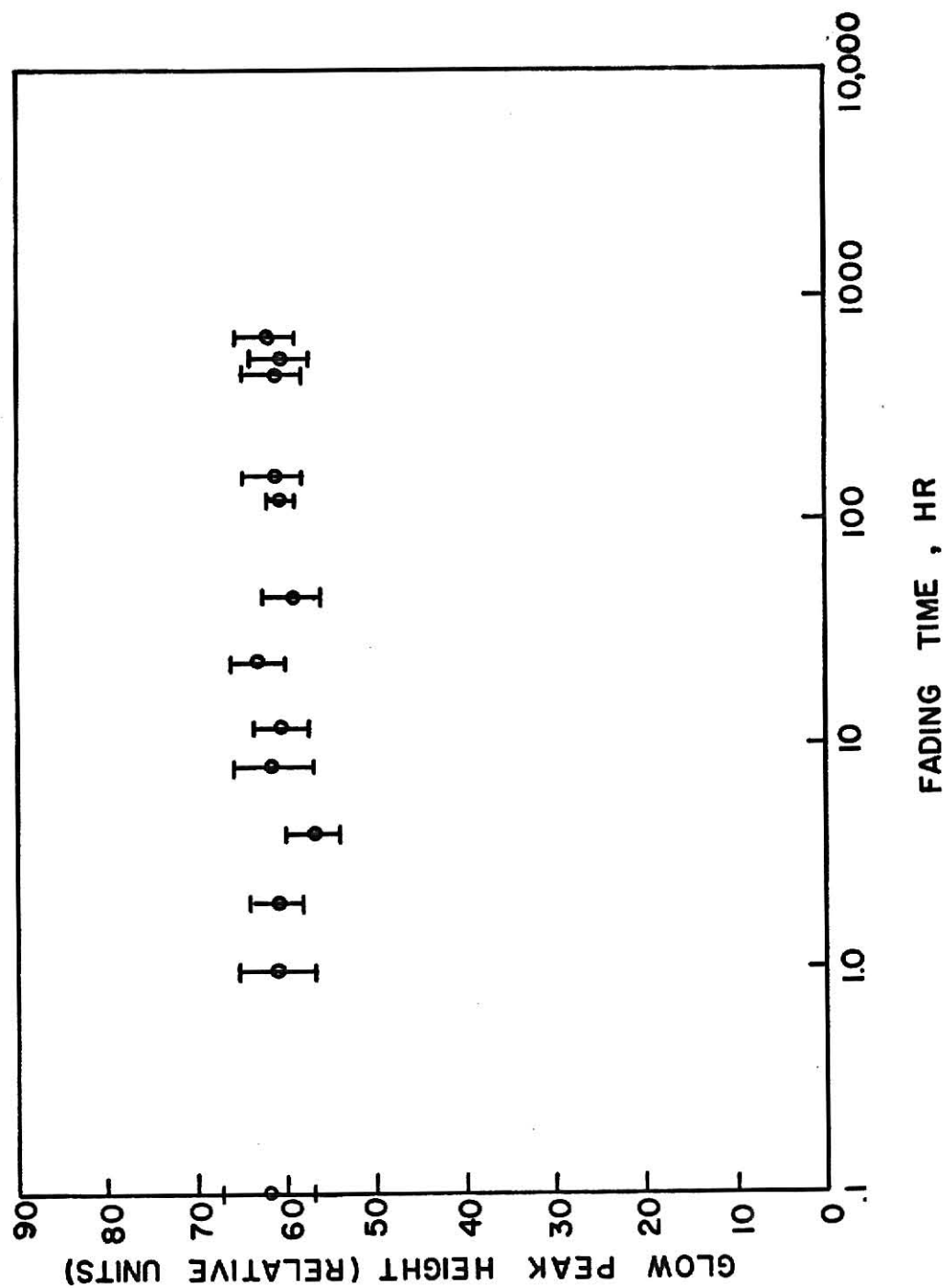


Figure 12. Long-term changes in the dosimeter (EG and G model TL-31) response with fading time.

Fig. 13. The shape of these data when plotted, indicate that there is more than one decay mechanism taking place.

The mathematical model used to fit the data was the sum of two exponentials. The model is as follows:

$$R = A_1 e^{-\left(\frac{.693t}{t_{\frac{1}{2}}^1}\right)} + A_2 e^{-\left(\frac{.693t}{t_{\frac{1}{2}}^2}\right)} \quad (2)$$

where

R = response from the reader,

A_1 = saturation activity of the first decay group,

A_2 = saturation activity of the second decay group,

$t_{\frac{1}{2}}^1$ = half-life of the first group,

$t_{\frac{1}{2}}^2$ = half-life of the second group,

t = decay time.

The standard technique of least squares would not work in this particular instance because the equations are non-linear. The equations were linearized by the Taylor's expansion keeping only the first term. An estimate of the various parameters was needed to get the first Taylor's expansion. After linearizing the equations, the least-squares analysis gave estimates of the parameters and these were used to expand in the Taylor's series for another least-squares estimate of the parameters.

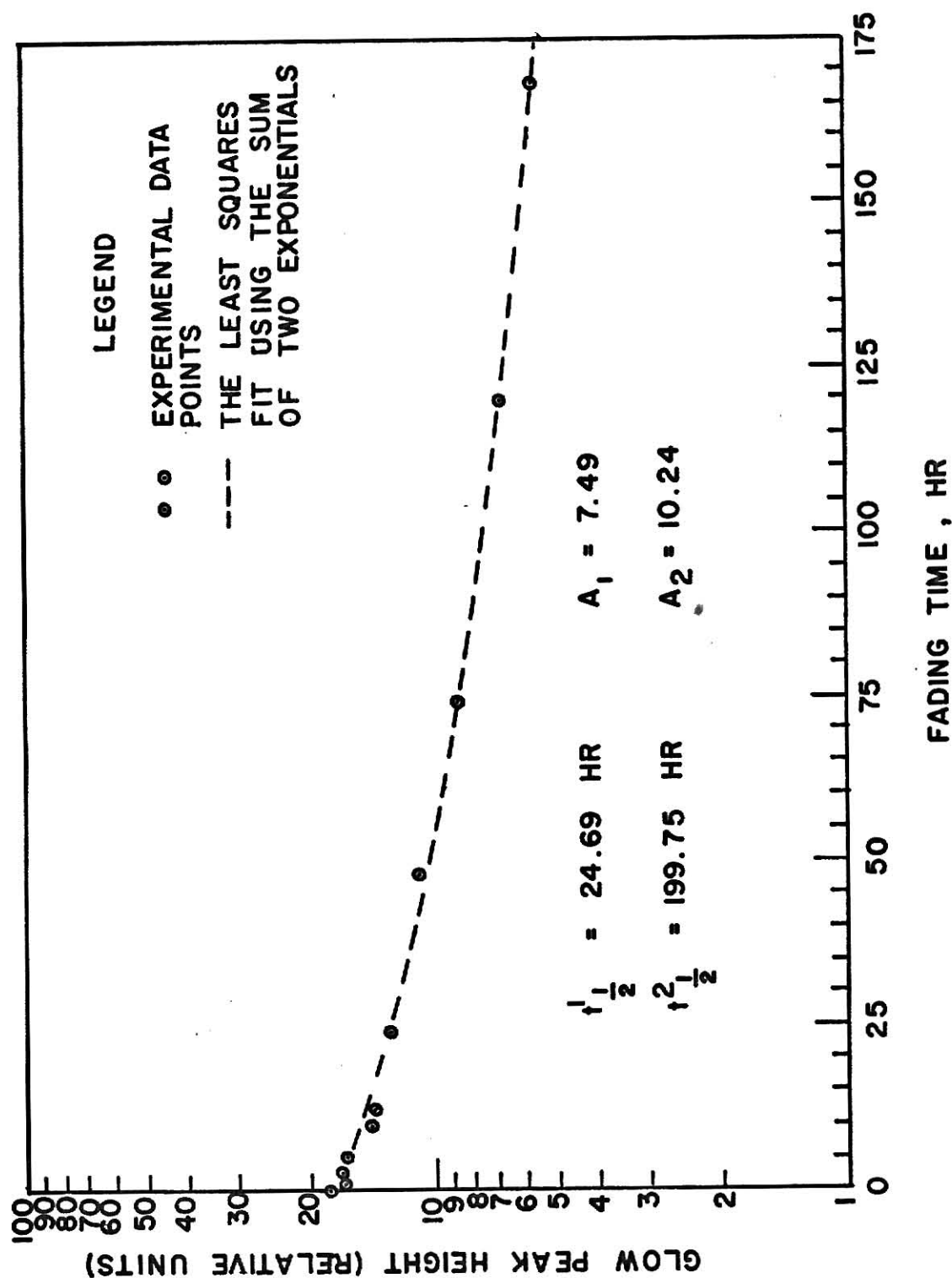


Figure 13. Loss of stored signal for the secondary glow curve peak using the EG and G TL-31 dosimeters. (The statistical deviations for the points were small and the error bars fell within the circles about the points; thus, they were not drawn on the graph.)

This interactive technique converged for the sum of two exponentials. A program was available in the Nuclear Engineering Department to fit the sum of several exponentials (10).

The values for parameters obtained for the first fit were (see Fig. 13 for the graph):

$$t_{\frac{1}{2}}^1 = 24.69 \text{ hr},$$

$$A_1 = 7.49 \text{ (relative units)},$$

$$t_{\frac{1}{2}}^2 = 199.75 \text{ hr},$$

$$A_2 = 10.24 \text{ (relative units)}.$$

The whole experiment on the fading of the secondary peak was repeated in order to obtain estimates of the standard deviations on the half-lives. There are more elaborate techniques for obtaining these estimates but it was not a primary objective of the experimenter to determine these standard deviations. The prime objective was to show that there are at least two decay mechanisms. The values obtained for the half-lives are:

$$t_{\frac{1}{2}}^1 = 21.16 \text{ hr},$$

$$A_1 = 4.34 \text{ (relative units)},$$

$$t_{\frac{1}{2}}^2 = 222.78 \text{ hr},$$

$$A_2 = 10.10 \text{ (relative units)}.$$

The average values are thus:

$$t_{\frac{1}{2}}^1 = 22.9 \pm 3.53 \text{ hr,}$$

$$A_1 = 5.91 \pm 3.15 \text{ (relative units),}$$

$$t_{\frac{1}{2}}^2 = 211.27 \pm 23.03 \text{ hr,}$$

$$A_2 = 10.17 \pm .14 \text{ (relative units).}$$

An attempt was made to fit the sum of three exponentials to these data by the same iterative technique as used previously, but the parameters would not converge. This indicates that there are only two decay schemes or that, if there is another decay scheme, it was so short-lived that these data were not taken frequently enough at the early period of decay. From Fig. 13, the sum of two exponentials appear to fit these data rather well.

6. DETERMINATION OF THE CALIBRATION CURVE

6.1. Necessity

The peak height obtained from the glow curve as plotted by EG and G reader is in relative units. A calibration curve is required to convert from the relative units to a radiation dose.

6.2. Equipment and Technique

The gamma-cell was used to irradiate the dosimeters for the calibration. The dosimeters were placed on the circumference of a two-inch diameter circle concentric with the outer diameter of a polyethylene disk, about 1/2-inch thick. The disk exactly fit in the irradiation chamber and allowed for several dosimeters to be irradiated at one time, all receiving the same dose because of their placement on an isodose. The disk provided a consistent positioning and holding device for uniformity of all irradiations. The isodose curve as supplied by the manufacturer was 2-3/4 inches above the base of the chamber and two inches from the axes in order to receive the dose equivalent to the dose at the center of the chamber. Polyethylene was used due to its small absorption property for gamma rays and the disk had already been constructed for use by previous experimenters.

The timer equipped on the gamma-cell was used to time the irradiation. The timer measured the time the plunger was at its lowest position only. Therefore, not only did the dosimeters receive a dose during the pre-set

time, but also some constant dose while the plunger was traversing down and on the way back up. Since the traverse time is a constant along with the dose rate, a constant dose, D_o , is received each time in addition to the dose received during irradiation of the pre-set time. Thus the total dose, D_t , is given by:

$$D_t = D_o + \dot{D}t \quad (3)$$

where \dot{D} is the dose rate in rads and t is the length of time irradiated.

Over the linear portion of the calibration curve, the total response, R , of the dosimeters in reader units is given by:

$$R = R_o + \dot{R}t \quad (4)$$

where R_o is the constant response due to traversing up and down in the cylinder and \dot{R} is the dose rate, in response units, of the gamma source. A weighted least-squares analysis on the experimental data was used to obtain estimates of R_o and \dot{R} . The calibration factor, cf , in units of rads per unit response can be determined by dividing the known value of the dose rate of the gamma-cell by the determined value \dot{R} . Thus, for over the linear region, the total response times the calibration factor gives the total dose received in rads.

6.3. Experimental Procedure

The dosimeters were first annealed at 350° for two hours and were left in the oven to cool slowly. After annealing, eight dosimeters

were irradiated to a given dose for each experimental point. In order to cover the large dose range from 200 rad to 5×10^5 rad for the calibration curve, these experimental points were approximately evenly spaced on a logarithmic scale. This was accomplished by back-calculations to determine the approximate time of irradiation for each experimental point. The dosimeters were all partially annealed for 7 minutes at 161°C , removed from the oven and allowed to cool for half an hour at room temperature before being read out.

6.4. Analysis of Data and Results

For each experimental point, the mean value and standard deviation was calculated. These values are presented in Table 1. The first five data points were used in the linear regression for estimating R_0 and \dot{R} . The values obtained from the linear regression were $R_0 = 11.42$ (relative units) and $\dot{R} = 3.53$ (relative units/sec). The calibration factor, cf, is obtained by dividing the known dose rate of 39.50 (rad/sec) by \dot{R} . Thus, the value obtained for cf was 11.18 (rad/relative unit). The calibration factor is for the linear portion from 0 to approximately 800 rad only.

The calibration factor times R_0 (the value obtained by linear regression) gives the additional dose, D_0 , of 127.62 rad. The estimated dose, D , is the dose rate multiplied by the exposure time and the total dose, D_t , is simply the sum of the additional dose and the estimated dose (see Eq. 3). The total doses are given in Table 1. In Fig. 14, the total

Table 1. Data and Results for the Calibration Curve

S. No.	Duration of irradiation t, sec.	Estimated dose* D, rad.	Total response R, units.	Total dose (D+D ₀), rad.
1	3	118.41	21.775 [±] .512	246.03
2	6	236.81	32.575 [±] .492	364.43
3	9	355.22	44.000 [±] .565	482.84
4	12	473.63	53.000 [±] .906	601.25
5	16	631.50	67.250 [±] 1.250	795.12
6	30	1184.07	128.50 [±] 3.39	1311.69
7	45	1776.11	210.75 [±] 5.41	1903.73
8	60	2368.14	283.75 [±] 7.07	2495.76
9	75	2960.25	375.50 [±] 5.14	3087.87
10	90	3552.21	469.38 [±] 8.52	3679.83
11	120 (2 min)	4736.28	686.3 [±] 8.2	4863.90
12	240 (4 min)	9472.56	1751.9 [±] 35.2	9600.18
13	360 (6 min)	14208.84	2996.3 [±] 65.3	14336.46
14	600 (10 min)	23681.40	5034.0 [±] 117.3	23809.02
15	840 (14 min)	33153.96	7550.0 [±] 192.7	33281.58
16	1200 (20 min)	47362.80	10763 [±] 267	47490.42
17	1800 (30 min)	71044.20	14675 [±] 508	71171.82
18	2400 (40 min)	94725.60	17575 [±] 288	94853.22
19	3600 (1 hr)	142088.40	16188 [±] 476	142216.02
20	7200 (2 hr)	284176.80	16781 [±] 288	284304.42
21	12600 (3.5 hr)	497309.40	14550 [±] 110	497437.02

*Estimated dose = (Dose rate in gamma-cell x Duration of irradiation).

Dose rate in the gamma-cell at the time of this experiment was 39.50 rad/sec.

dose is plotted as the abscissa and the respective experimentally determined points as the ordinate for the calibration curve.

The calibration curve indicated supralinearity (an essentially nonlinear effect) with respect to dose above approximately 10^3 rad. To obtain a better idea of the supralinearity, a weighted least-squares analysis was used to fit a straight line through the first five data points and another through the next eleven data points. The values for the linear equation obtained for the first five data points were: slope = $0.0864 \pm .0019$ (relative unit/rad) and the y-intercept = 1.088 ± 0.827 (relative units). The values for the linear equation of the next eleven data points were: slope = $0.1794 \pm .0016$ (relative units/rad) and the y-intercept = -138.52 ± 4.25 (relative units). The slope of the straight line fitted to the eleven data points above 10^3 rad is twice the slope of the straight line below 10^3 rad. The supralinearity is not vividly illustrated on the logarithmic graph. The plot of the straight line fitted to the eleven experimental data points above 10^3 rad is shown in Fig. 14 (plotted on a logarithmic graph) as the "dashed line curve." The straight line fitted to the five experimental data points below 10^3 rad is so near the actual calibration curve in that region that the curve was not plotted in Fig. 14.

The solid line curve in Fig. 14 is simply a smooth curve drawn through the experimental data points for the calibration curve. The calibration curve was extended to very high dose until saturation was reached. Saturation was reached at a dose of about 10^5 rad. This seems

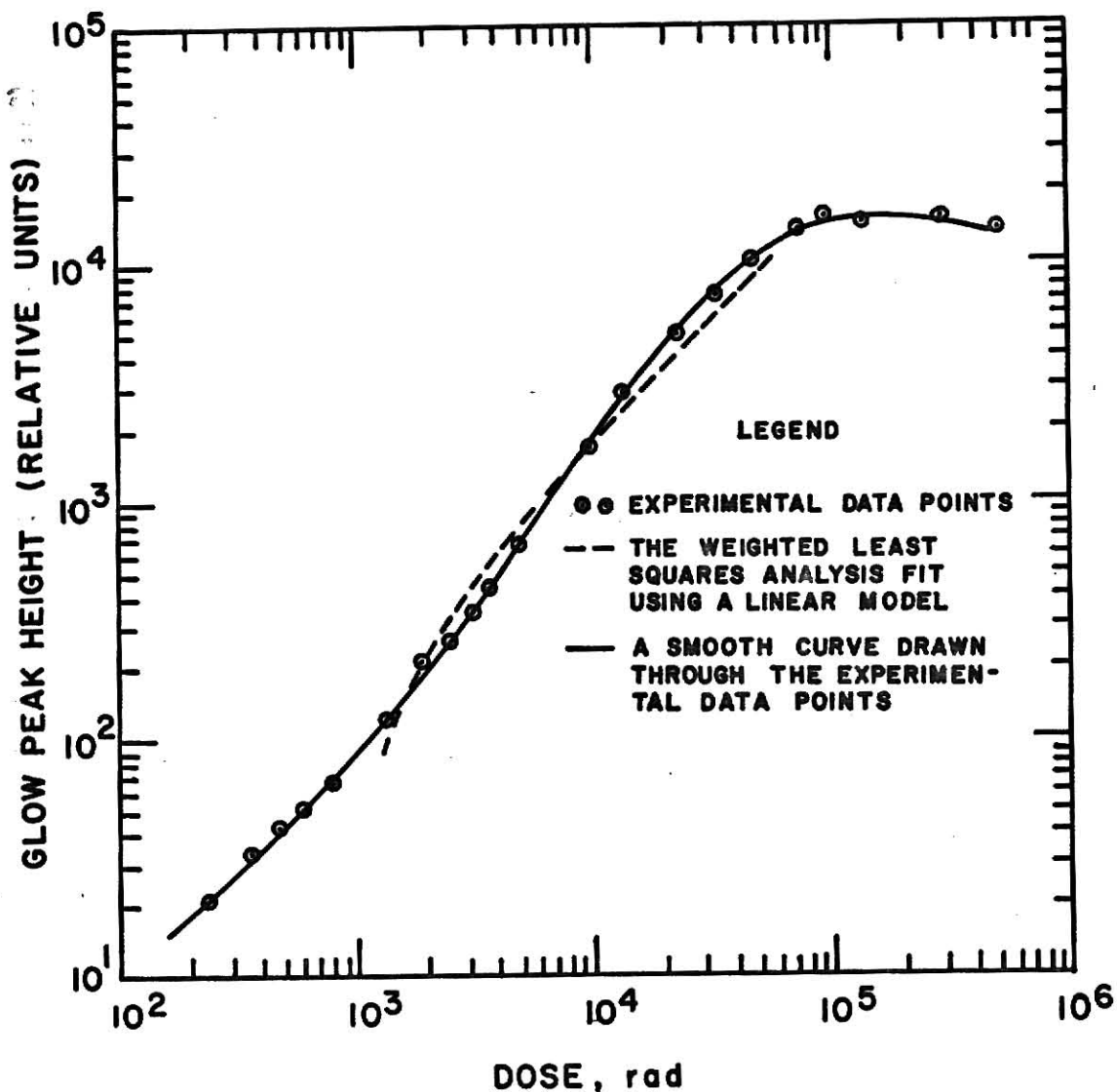


Figure 14. The calibration curve for the EG and G model TL-31 $\text{CaF}_2\text{:Mn}$ dosimeters. The dosimeters were partially annealed after irradiation at 161°C for 7 minutes. (The statistical deviations for the points were small and the error bars fell within the circles about the points; thus, they were not drawn on the graph.)

to be somewhat lower than the value reported by EG and G (9). They report the useful range of calcium fluoride mini as approximately 20 mR to 5×10^5 R.

The dosimeters that reached saturation seem to have sustained radiation damage. Eight dosimeters were annealed overnight to insure all the traps had been emptied. All eight had previously been irradiated to saturation. They were left in the annealing oven to cool slowly. They were all irradiated for 30 sec in the gamma-cell. Before being read out, the dosimeters were partially annealed at 161°C for 7 min and then cooled at room temperature for 30 min. Upon being read out, an average response of 300.38 ± 14.96 (relative units) was obtained for the eight dosimeters. This is significantly higher than the value of 128.50 ± 3.39 (relative units) obtained in the calibration data. The fact that the sensitivity more than doubled indicates a presence of more imperfections. Traps must have been created due to radiation damage in reaching saturation. The radiation damage investigation was not carried any further. It was only of interest, at this time, to see if radiation damage was indicated.

7. SUGGESTIONS FOR FUTURE STUDY

From the results obtained in this research, there are suggested several areas of possible investigation. One area is the discrepancy between Schulman's work and these fading study results for the primary peak of the $\text{CaF}_2\text{:Mn}$ dosimeters. This difference could be in the impurity doping which may be related to the secondary peak that was not reported as having been observed previously. Thus, these two discrepancies could be closely related and are both areas for future investigation. Also connected with the fading studies would be a study of the manner in which the heating rate affects the fading properties of the primary peak, if at all.

Another conceivable area of investigation is the supralinearity observed in the calibration curve. This shows there are some non-linear effects which are not readily explainable and would be of interest for an investigation.

The radiation damage observed in the saturation region is another obvious area of further study. The type of radiation damage and the extent of the damage are of interest here.

The last extension of this research would be a dose-rate study. This area is presently under investigation by another graduate student in the Nuclear Engineering Department here at Kansas State University.

8. ACKNOWLEDGEMENTS

The author is indebted to a number of people: to Dr. Hermann J. Donnert for his continuous guidance and help; to Dr. N. D. Eckhoff for his guidance on the statistical analysis of the data; and to Mr. Ray E. Hightower for his help with the experimental equipment and preparation of thesis.

The fellowship grant from the Office of Civil Defense and the financial support from the Department of Defense Themis Project, administered through the Office of Naval Research, are gratefully acknowledged.

9. LITERATURE CITED

1. Spurny, Z., "Thermoluminescent Dosimetry," At. En. Rev., Vol. 3, No. 2, 61, 1965.
2. Schulman, J. H., "Survey of Luminescence Dosimetry," CONF-650637, AEC Symposium Series, 8, 16, 1967.
3. Blizard, E. P., Reactor Handbook, Interscience Publisher, New York, 1962.
4. Spinks, J. W. T. and R. J. Woods, An Introduction to Radiation Chemistry, John Wiley & Sons, Inc., New York, 1964.
5. Ginter, R. J. and R. D. Kirk, "The Thermoluminescence of $\text{CaF}_2:\text{Mn}$," J. Electrochem. Soc. 104:365, 1957.
6. Cameron, J. R., N. Suntharalingam and G. N. Kenney, Thermoluminescent Dosimetry, University of Wisconsin Press, Madison, 1968.
7. Kaiserudden, M., "Effects of Very High Dose Rates of the Response of LiF Thermoluminescent Dosimeters," M.S. Thesis, Kansas State University, Department of Nuclear Engineering, 1968.
8. Brownlee, K. A., Statistical Theory and Methodology, John Wiley & Sons, Inc., New York, 1967.
9. "TL Dosimetry System, Models TL-38 and TL-3C," Operation Manual, #S-316-MN, EG and G Santa Barbara Division, 1966.
10. Thiesing, J. W., "Experimental Measurement of Delayed Neutron Parameters for U^{235} ," N. E. 851 Report, August 1969.
11. Bliss, C. E., "The Response of ^6LiF and ^7LiF Thermoluminescent Dosimeters to Neutron and Gamma-Radiation Dose," M.S. Thesis, Kansas State University, Department of Nuclear Engineering, 1967.

THE RESPONSE CHARACTERISTICS OF
 $\text{CaF}_2\text{:Mn}$ THERMOLUMINESCENT DOSIMETERS

by

ALBERT JOHN ALEXANDER

B.S., Kansas State University, 1969

AN ABSTRACT OF A MASTER'S THESIS

submitted in partial fulfillment of the

requirements for the degree

MASTER OF SCIENCE

Department of Nuclear Engineering

KANSAS STATE UNIVERSITY
Manhattan, Kansas

1970

ABSTRACT

The theory of thermoluminescence and thermoluminescent dosimetry was reviewed. A pre-irradiation procedure of heating the dosimeters at 350°C for 2 hours was decided upon for all dosimeters. A post-irradiation annealing procedure of 7 min at 161°C followed by readout one-half hour later was found experimentally to be beneficial in reducing the spread of the data.

Long-term fading studies were done for the secondary and primary peak at room temperature. In the primary peak fading studies, one of the studies included post-irradiation annealing while the others did not.

A calibration curve for ^{60}Co gamma radiation in the dose range (10^2 to 5×10^5 R) was determined for the model TL-31 thermoluminescent dosimeters.

Conclusions drawn from the analysis of data were:

1. The post-irradiation process reduced the spread of the data.
2. There are at least two decay schemes in the fading at room temperature of the secondary peak observed in the model TL-31 dosimeters.
3. There is no fading of the primary peak at room temperature for the model TL-31 dosimeters.
4. There is supralinearity above 10^3 rad in the calibration curve.
5. Saturation was reached at 10^5 rad in the calibration curve.